www.czasopisma.pan.pl PAN POLSKA AKADEMIA NAUK www.journals.pan.pl

Arch. Metall. Mater. **64** (2019), 2, 443-450

DOI: 10.24425/amm.2019.127558

G. DERCZ*#, I. MATUŁA*, W. GURDZIEL*, N. KUCZERA*

MICROSTRUCTURE EVOLUTION OF Ti/ZrO_2 AND Ti/Al_2O_3 COMPOSITES PREPARED BY POWDER METALLURGY METHOD

The current study were performed in order to assess the fabrication possibility of the metal-ceramic composites based on nanocrystalline substrates. The influence of the variable time of the high energy ball-milling (10, 30 and 50 h) on the structure, pores morphology and microhardness of Ti/ZrO_2 and Ti/Al_2O_3 compositions was studied. The X-ray diffraction analysis confirmed the composite formation for all milling times and sintering in the case of Ti/ZrO_2 system. Decomposition of substrates during milling process of Ti/Al_2O_3 system was also observed. Additionally, the changes of lattice parameter as a function of milling time were studied. The morphology of powders and the microstructure of the sintered samples were observed by scanning electron microscopy (SEM). Also, analysis of microhardness and pores structure were performed.

Keywords: composite, Ti-ZrO_2, Ti-Al_2O_3, high energy ball milling, Rietveld analysis

1. Introduction

Due to increasing demand from bone implants and non-perfection of current use materials the new classes of biomaterials are developing [1,2]. The one way of development is a fabrication of nanocomposites as materials for long lasting bone implants. In these materials the ceramic nanoparticles are dispersed in the metallic matrix, what induces the strengthening effect on the material. The dispersed nanoparticles are superior to micro-dispersion strengthening in monolithic alloys [3,4]. The unique properties of nanocrystalline materials are related to a large number of grain boundaries compared with polycrystalline coarse-grained particles [5]. The titanium and titanium-based alloy seem to be the most attractive metallic material for orthopaedic long-lasting applications and dental implants. This material is characterized by the ability to self-passivation and high corrosion resistance in comparison to other metallic materials [2,6]. However, almost all metallic biomaterials have poorer bioactivity in comparison to bioceramic [7]. That situation can be improved by the dispersed nanoparticles (like Al_2O_3, ZrO_2) which are characterized by inert in the environment of living tissues. The application of ZrO_2 is motivated by high strength, high bending strength, abrasion resistance, resistance to thermal shock, biocompatibility and low affinity to bacterial colonization [8-11]. The α-Al_2O_3 as a dispersed phase offers improvement of strength, resistance to thermal shock and chemical stability, and at the same time it is relatively low cost nanomaterial [12,13]. Another important aspect of materials for long lasting implants is the mechanical properties mismatch between the bone and material of implant. It has been noted that the pores in strict defined structure and sizes, has an actual influence on mechanical properties (strength, Young modulus and also fatigue life) of the material [14,15]. Moreover, the porous surface of an implant and the presence of ceramic can promote the bone cells ingrowth into the pores, which can improve the connection between an implant and the bone [16]. It is expected that the porous titanium-ceramic composites will exhibit mechanical properties of titanium and excellent biocompatibility, low wear rate of ceramics.

In the present study, the possibility of fabrication of Ti/ZrO_2 and To/Al_2O_3 composites using a combination of high energy ball milling (HEBM) and sintering methods were assessed for their potential biomedical application. The use of milling will be helpful for nanocrystallization [17] of the initial substrates and to obtain a powder with various grain size distribution. This will influence the presence of pores and changes of phase composition and some mechanical properties in sintered composites. In the presented studies the influence of the time of HEBM on phase composition, structure, porosity and microhardness of sintered composites will be shown.

2. Experimental details

The of nominal compositions Ti/Al_2O_3 and Ti-10ZrO_2 (wt.%) were prepared using the commercial powders: Ti (Atlantic Equipment Engineers (AEE), 99.7%, <45 μm), Al_2O_3

* UNIVERSITY OF SILESIA IN KATOWICE, INSTITUTE OF MATERIALS SCIENCE, 1A 75 PUŁKU PIECHOTY STR, 41-500 CHORZÓW

Corresponding author: grzegorz.dercz@us.edu.pl

(POCH, 99.9%, <44 μm) and ZrO_2 (Atlantic Equipment Engineers (AEE), purity 99.9%, <44 μm). At the first stage the nanocrystalline powders were prepared by high-energy milling in a Fritch Pulverisette 7 premium line planetary-ball mill an Ar protective-gas atmosphere [18]. The green compacts were prepared by cold isostatic pressing under 1000 MPa pressure and after that were sintered at 900°C for 12 h. The sample labels are present in table 1.

TABLE 1

The samples designations, which were used in text depend on composition and milling time

After milling			
Composition	**Time of milling**		
	10h	**30h**	**50h**
Ti/Al_2O_3	T-A10	T-A30	T-A50
Ti/ZrO_2	T-Z10	T-Z30	T-Z50
After milling and sintering			
Composition	**Time of milling**		
	10h	**30h**	**50h**
Ti/Al_2O_3	T-A10+HT	T-A30+HT	T-A50+HT
Ti/ZrO_2	T-Z10+HT	T-Z30+HT	T-Z50+HT

The phase content was studied by X-ray diffraction (XRD) with the use of a Phillips X'Pert X-ray diffractometer. The Rietveld analysis was performed applying DBWS-9807 program that is an update version of the DBWS programs for Rietveld refinement with PC and mainframe computers [19]. The microstructure of sintered samples and fractured surfaces were observed using the scanning electron microscope (SEM) JEOL JSM 6480 with the accelerating voltage of 20 kV. Additionally, the chemical analysis was performed using the energy dispersive X-ray spectroscopy (EDS) detector manufactured by IXRF. The fractured surfaces of composites for SEM analysis were revealed as a result of breaking of the sintered discs.

The analysis of porosity was performed by image analysis using the ImageJ software and the planimetric method on a total area of ~1.3 mm^2 for each sample. The assessment of the pores size was carried out by the stereological parameters: volume fraction of the pores V_V [%], ($V_V = \frac{N_p}{N_o}$ (1), where N_p – number of pixels of the pores being analyzed; N_o – the image total number of pixels) and Feret's diameter as the longest distance between two points along the pores. Also, were assessed the pores shape by dimensionless shape factor – of the circularity ($f_p = \frac{4 \cdot \pi \cdot F}{L^2}$ (2), where: F – analyzed object area ; L – analyzed object perimeter). Mechanical properties were tested by microhardness measurements by Wolpert Micro Vickers tester 401MVD with the load of 500 N and loading time of 10 s.

3. Results and discussion

The XRD analysis of Ti/Al_2O_3 composition after all milling time revealed the presence of α-Ti, Al_2O_3 phases. Additionally, for the sample after the longest milling time the presence of TiO phase was detected (Fig. 3). The morphology of Ti/Al_2O_3 and Ti/ZrO_2 powders after high-energy milling (for 10 h, 30 h and 50 h) is shown in SEM micrographs (Fig. 1). The change of powder morphology dependent on milling time and type of dispersion

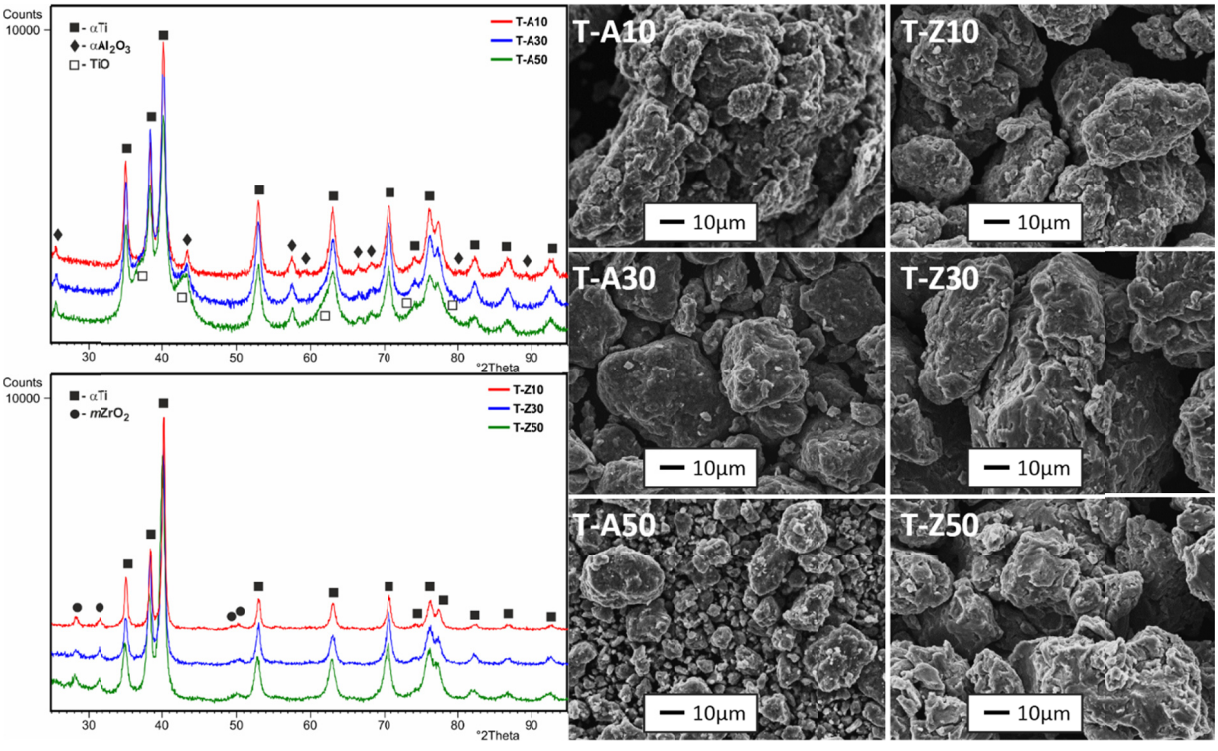

Fig. 1. X-ray diffraction patterns and SEM micrographs of T-A10, T-A30, T-A50, T-Z10, T-Z30 and T-Z50 samples

phase were clearly visible. In the case of Ti/Al_2O_3 composition the particles size were decreasing with increasing milling time. The shape of received particles become more globular simultaneously with longer milling time . In contrast, for Ti/ZrO_2 composition firstly partial fragmentation was observed, but for longer milling time the agglomeration of powder and increase of particles size was observed. The particles shape was irregularl, furthermore portions of material welded on particles were observed. Such particles size and shape changes are a result of characteristic processes occurring during milling. For Ti/ZrO_2 composition the predominance of cold welding over the hardening and fracturing was observed with increasing milling time. Generally during mechanical alloying particles are repeatedly flattened, cold welded, fractured and rewelded. That changes of material confirmed the dominance of particularly processes depending on composition, more specifically of starting materials characteristic, in this case, of dispersive phase [20,21].

In the case of Ti/Al_2O_3 system after all milling times the analysis revealed the presence of αTi and Al_2O_3 phases (Fig. 1). Additionally, for the sample after the longest milling time the presence of TiO phase was detected. For T-A10+HT sample after sintering Ti, Ti_3O and Ti_3Al phases were detected, however for samples T-A30+HT, T-A50+HT the following phases: Ti_3Al and Ti_3O were detected. In the case of this composition the obtained material was not the desired composite, because as final effect of milling and sintering new phases were obtained, different from initial material. Mas-Guindal et al. [22] also received $TiAl_3$ phase during producing cermets through activated SHS reaction and was found in a region adjacent to interface in Ti/Al_2O_3 as an effect of interaction between molten titanium and Al_2O_3 [23]. The $TiAl_3$ phase was created according to Ti-Al phase diagram [24] as an effect of earlier decomposition of Al_2O_3 during the milling. The presence of Ti_3O phase can be explain as part of a reaction layer, which may be controlled by the kinetics system in Ti/Al_2O_3 material [25]. In the case of the Ti/ZrO_2, the XRD analysis on both stages of producing process revealed phases identical to starting phases regardless of milling time. The metal-ceramic composite was successfully obtained by powder metallurgy method.

Based on the diffraction patterns of obtained samples and the Rietveld refinements the lattice parameters were determined for Ti/Al_2O_3 (Tab 2.) and Ti/ZrO_2 (Tab. 3) compositions. In the case of Ti/Al_2O_3 samples the increase of lattice parameters

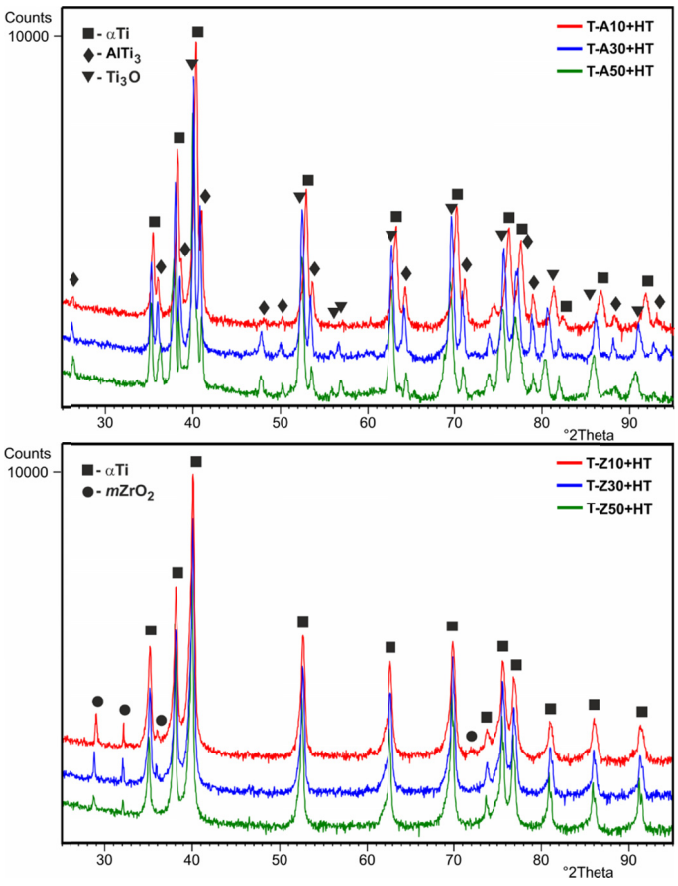

Fig. 2. X-ray diffraction patterns of the Ti/Al_2O_3 and Ti/ZrO_2 systems after sintering

of Ti_3O and Ti_3Al phases whit increasing milling time was observed. The expansion of Ti_3O unit cell was connected with the creation of oxides. It should be highlighted that in sample T-A50 for Ti_3Al phase the parameters of unit cell were close to the reference ICDD data. It could be connected with the size of particles obtained in milling processes. The increase of milling time leads to better homogenization of sintered samples as an effect of the occurrence of more boundaries, thereby the easier diffusion. The Rietveld analysis revealed no significant changes of lattice parameters in the case of Ti/ZrO_2 composition. A slight decrease of a_0 parameters with simultaneously decrease of c_0 parameter of $mZrO_2$ phase was observed.

Figure 3 shows the microstructure of the sintered samples for both compositions. For all samples the microstructure were

TABLE 2

Unit-cell parameters of phases of the Ti/Al_2O_3 system after sintering the samples with various milling time

Composition	Phase	Lattice parameter [nm]					Types of changes
		Unit-cell parameter [nm]	ICDD*	Sample			
				T-A10+HT	T-A30+HT	T-A50+HT	
Ti/Al_2O_3	αTi	a_0	0.2950	0.29513(3)	—	—	↑
		c_0	0.4682	0.46529(2)	—	—	↓
	Ti_3O	a_0	0.5141	0.51106(3)	0.51318(2)	0.51501(4)	↑
		c_0	0.9533	0.95271(1)	0.95384(6)	0.95409(5)	↑
	Ti_3Al	a_0	0.5813	0.58073(7)	0.58095(4)	0.58121(3)	↑
		c_0	0.4713	0.46936(9)	0.47059(5)	0.47094(3)	↑

TABLE 3

Unit-cell parameters of phases of the Ti/ZrO_2 system after sintering the samples with various milling time

Composition	Phase	Lattice parameter [nm]					Types of changes
		Unit-cell parameter [nm]	ICDD*	Sample			
				T-Z10+HT	T-Z30+HT	T-Z50+HT	
Ti/ZrO_2	αTi	a_0	0.2950	0.29572(2)	0.29574(3)	0.29574(2)	—
		c_0	0.4682	0.46886(3)	0.46884(2)	0.46883(5)	—
	$mZrO_2$	a_0	0.5298	0.52792(1)	0.52788(4)	0.52781(3)	↓
		b_0	0.5216	0.52106(5)	0.52116(4)	0.52125(2)	↑
		c_0	0.5115	0.52085(5)	0.52099(3)	0.52091(4)	—

composed of connected particles, which were a result of milling processes. In the material two types of connections between the particles were observed. In the first type, the particles were connected as an effect of compression each other during cold isostatic pressing (Fig. 3 – dotted line). The second type of connection had a permanent character because there were observed neck between particles, which were created during the sintering by diffusion processes (Fig. 3. – solid line). It was clearly visible that obtained microstructure depends on the shape and size of powders obtained as a result of milling processes. The milling time has a significant influence on material obtained after sintering [26]. For Ti/Al_2O_3 composition the microstructure becomes finer with increasing milling time, a simultaneously smaller number of permanent connections between particles were observed. This observation correlated also with XRD analysis of powders after milling. It can be concluded that the presence of TiO phase on the particles surface made the diffusion impossible, what resulted in not permanent connection between particles. In the case of Ti/ZrO_2 the microstructure was similar independent from the milling time. Additionally, based on optical microscope micrographs the porosity analysis of sintered samples was performed. The analysis was focused on the optimal size and structure of the pores for improved osseointegration between the implant and human bone. The total porosity were presented in table 4. For both compositions the increase of porosity with increasing milling time was observed. Additionally, the high pores percentage have an influence on mechanical properties of the material – it decreases the elastic modulus of material [14,27]. Furthermore, based on stereological analysis it was observed that the T-A30+HT and T-A50+HT samples possess relatively large porosity (over 60 %), what could be an effect of two aspects. First, the distribution of particles in 3d space could build an extended skeleton, what would be great achievement in relation to potential better osseointegration. The second reason of such results could be decomposition of surface during the preparation of samples by mechanical grinding and polishing, as results of not strong enough connection between the particles. Additionally, the percentage of pores with predefined Ferret's diameter was assessed. The optimal pore size for osseointegration in the literature were estimated between 50 and 500 µm [28,29]. In the case of Ti/Al_2O_3 system the content of pores with Ferret's diameter in this range, decreased from over 10.0% to 1.6% with increasing milling time . For Ti/ZrO_2 system a higher content of pores with an optimal size for each milling time were notice. Sample T-Z30+HT showed the highest pores percentage (almost 25.0%) of which Ferrets diameter were in 50-500 µm range. This observation and fact of obtaining the composite let to the conclusion that this sample is the best candidate for further researches as potential material for long-lasting bone implants. Additionally, the pores shape were assessed by circularity factor. The differences between the samples were negligibly small and did not show any dependence on composition or milling time. In researched were mentioned the influence of milling parameters on pore structure of obtained samples [26,30], also in case of composites was confirmed.

TABLE 4

Total porosity, pores Feret's diameter in pre-defined ranges and pores circularity for all samples depend on composition and milling time

Samples	Porosity [%]	Feret's diameter [%]			Circularity
		<50 µm	50-500 µm	>500 µm	
T-A10+HT	19	89.4	10.6	0.0	0.5
T-A30+HT	62	96.1	3.5	0.4	0.4
T-A50+HT	65	94.8	1.6	3.6	0.5
T-Z10+HT	19	90.7	9.3	0.0	0.4
T-Z30+HT	22	75.1	24.9	0.0	0.4
T-Z50+HT	35	93.0	6.5	0.4	0.5

The complementary researched were EDS analysis, which allows to the designation of distribution maps of elements performed for all samples after sintering. Both studied systems showed a regular distribution of titanium in the analyzed area. However, the distribution of Al and O were irregular in Ti/Al_2O_3 sample (Fig. 4). First of all the parameters of milling have a significant influence on homogenization of milled material. Another aspect is an interface interaction between Ti and Al_2O_3 particles. The regions enriched in Al could lead to the formation of $AlTi_3$ [31]. In the case of Ti/ZrO_2 system the more regular distribution of Zr and O was observed, what was further improved by increasing milling time (Fig. 4). The performed analysis confirmed that every particles building up the structure was well balanced material with preserved stoichiometry.

The morphology of fracture surfaces were also analyzed (Fig. 5). The fracture mode of T-A10+HT is predominantly transgranular, what indicates the brittle fracture of sample,

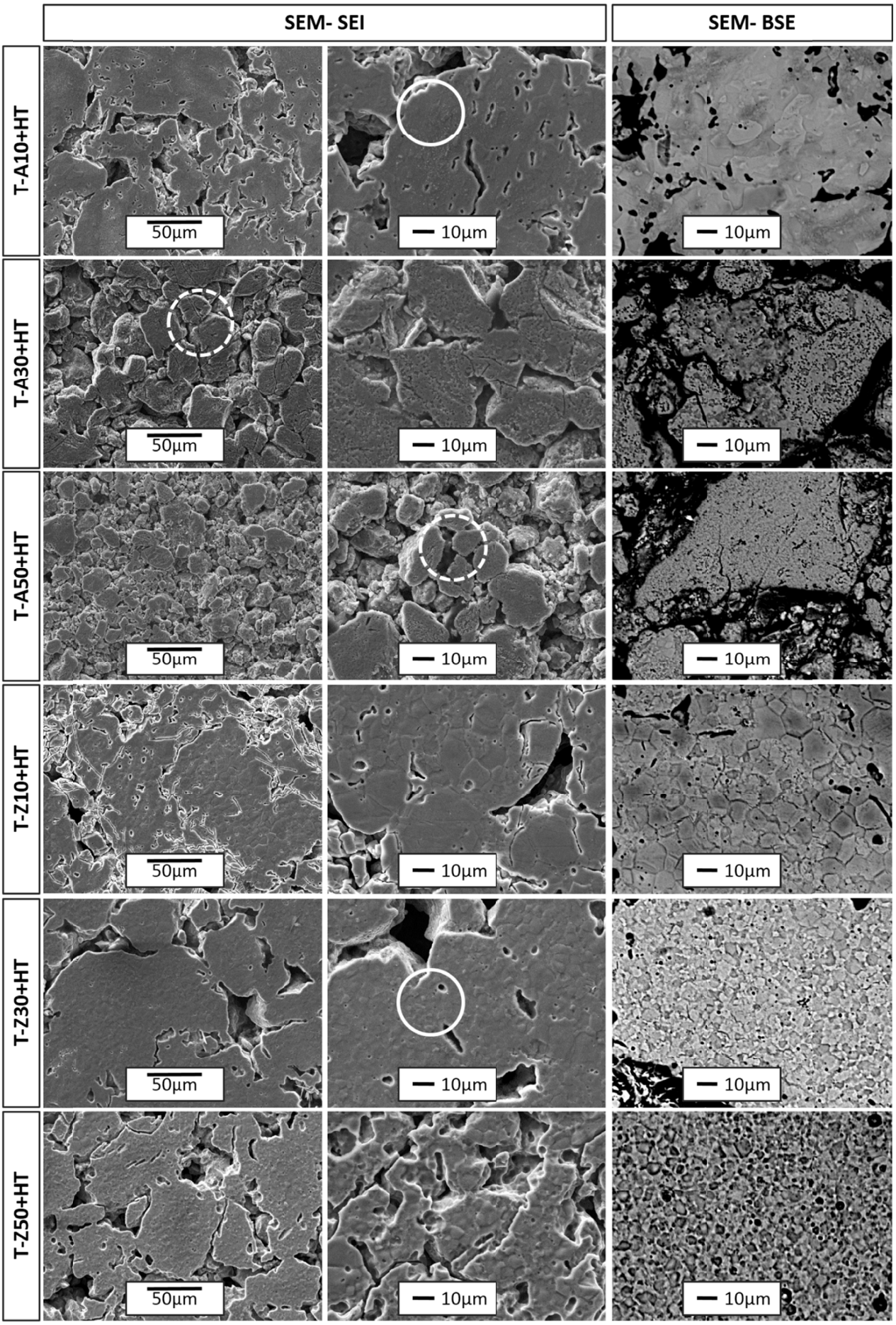

Fig. 3. SEM (SEI and BSE mode) micrographs of samples after sintering

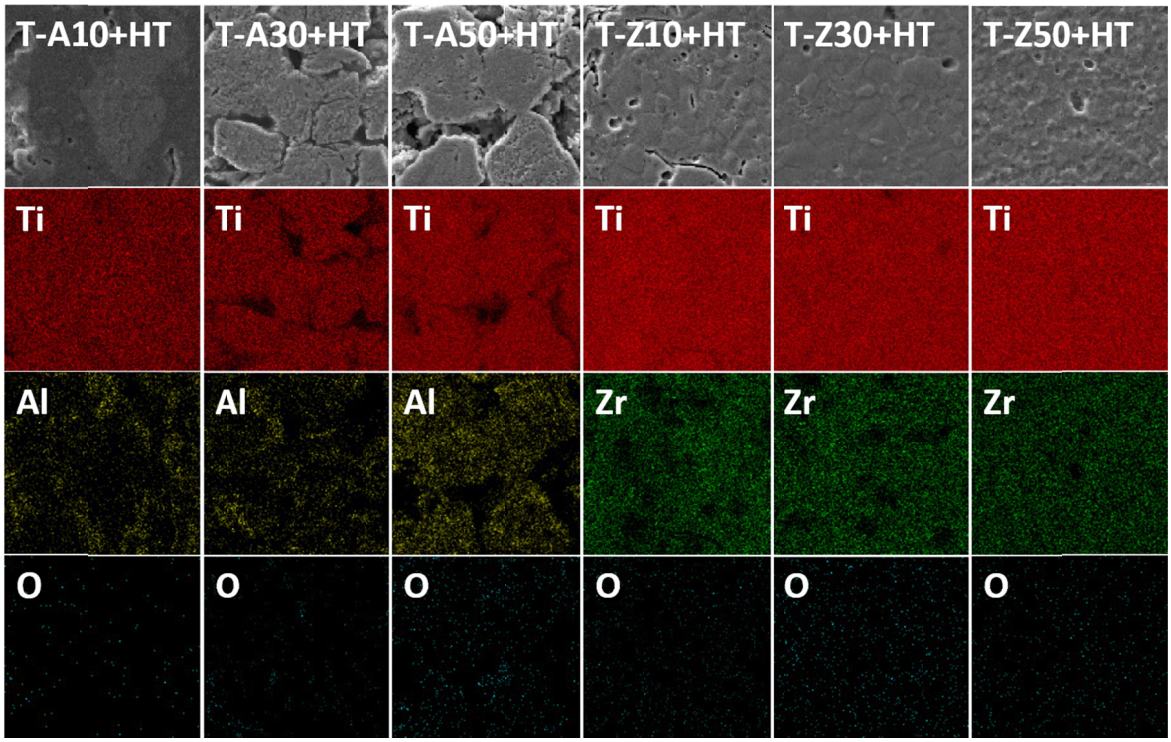

Fig. 4. Elemental distributions maps of T-A10+HT, T-A30+HT, T-A50+HT, T-Z10+HT, T-Z30+HT and T-Z50+HT samples

however for next two samples in this composition whole grains, intergranular fractures, without signs of brittle fracturing were observe. That situation could be an effect of oxides presence on particles surface after milling or an insufficiently strong connection between each particles. The analysis of fracturing of Ti/ZrO_2 samples reveals the tendency of this material to create agglomerates and brittle fracture. The brittle fracture is a complex function of many parameters, which include: material density, the grain size of the matrix, type, proportion and size of reinforcing particles, state of intergranular and interphase boundaries and state of stress in reinforcing particles and their surroundings.The presence of brittle fracture in Ti/ZrO_2 samples can be explain by internal stress and presence of *m*ZrO_2 nanocrystalline particles. However, the mechanically stability of *m*ZrO_2 was achieved by incorporation with Ti particles, which concentration was slightly over the percolation threshold [32,33].

The microhardness measurement were the first look at mechanical properties (Fig. 6). It is clearly seen that the microhardness of Ti/Al_2O_3 system decreases with increasing milling time, what was connected with the structure of sintered material as it is shown in figure 6. For sample T-A10 the measurement was performed in solid area, however for sample T-A50+HT it was impossible to pick up such regions for measurements because the microstructure of the sample was different. Additionally, the results could be an effect of not stable connection between particles in the sample. For composition Ti/ZrO_2 the microhardness increase with increasing milling time , what can be referred to processes of hardening of powder during the ball milling. This effect could be directly related to obtaining of finer microstructure and nanostructure [20,34].

4. Conclusion

In the present study the possibility of porous Ti/Al_2O_3 and Ti/ZrO_2 composites fabrication using a combination of high energy ball milling and sintering methods was assessed. The studies lead to the following conclusions:

- Change of phase composition and initial powder morphology of substrates dependent on milling time and type of dispersion phase.
- Decomposition of substrates during milling of Ti/Al_2O_3 composition is observed.
- The effect of previously high-energy milling process of the substrates on the structure, phase composition, porosity and microhardness of the sintered Ti/ZrO_2 and Ti/Al_2O_3 composites were observed.
- Studies confirmed the possibility to obtain Ti/ZrO_2 composite from nanocrystalline substrates.
- For compositions of Ti/ZrO_2 and Ti/Al_2O_3 the microhardness respectively increase and decrease with increasing of milling time.
- The T-Z30+HT sample represent the balance between porosity structure and mechanical properties, what indicate this sample for the most optimal for potential biomedical uses in compare to other samples.

Acknowledgements

This work was supported by the Polish National Science Centre (Polish: Narodowe Centrum Nauki, abbr. NCN) under research project nos. 2011/03/D/ST8/04884 and 2016/23/N/ST8/03809.

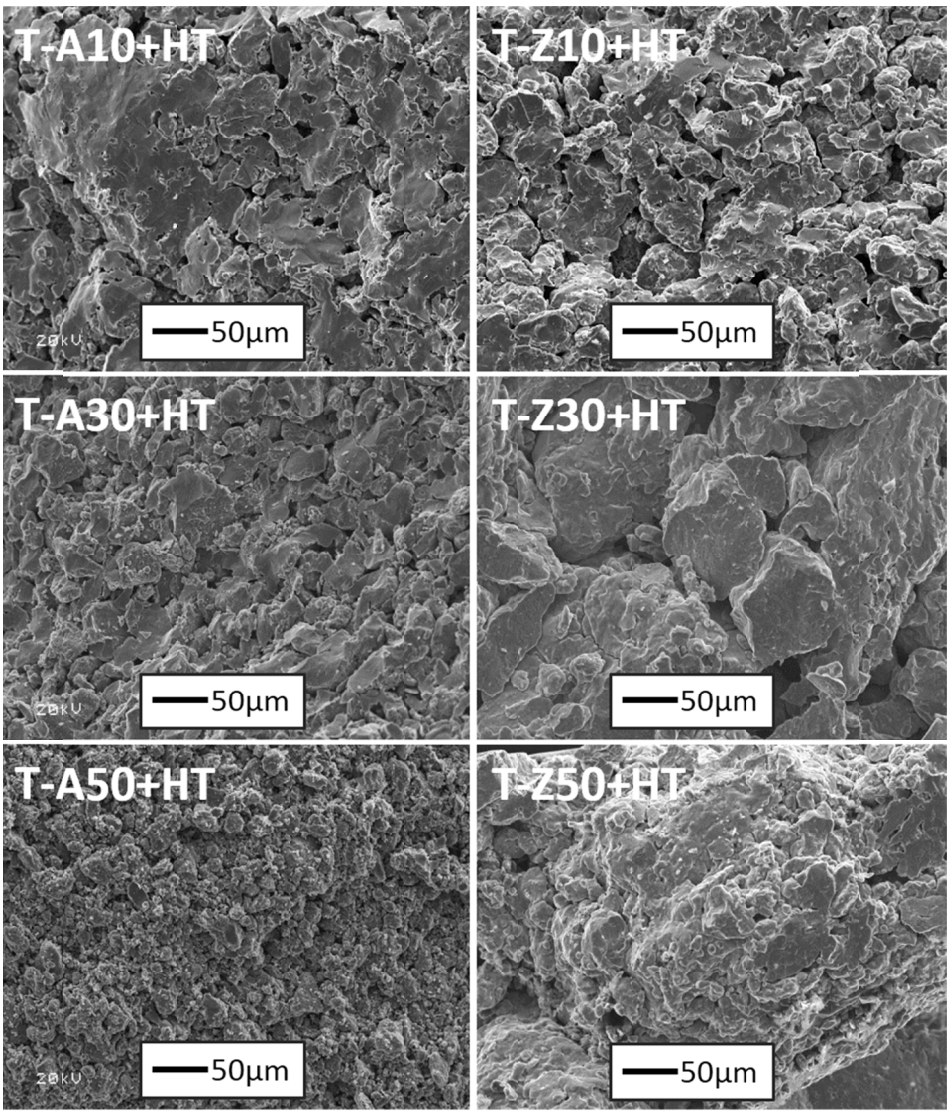

Fig. 5. Fracture surfaces of T-A10+HT, T-A30+HT, T-A50+HT, T-Z10+HT, T-Z30+HT and T-Z50+HT samples

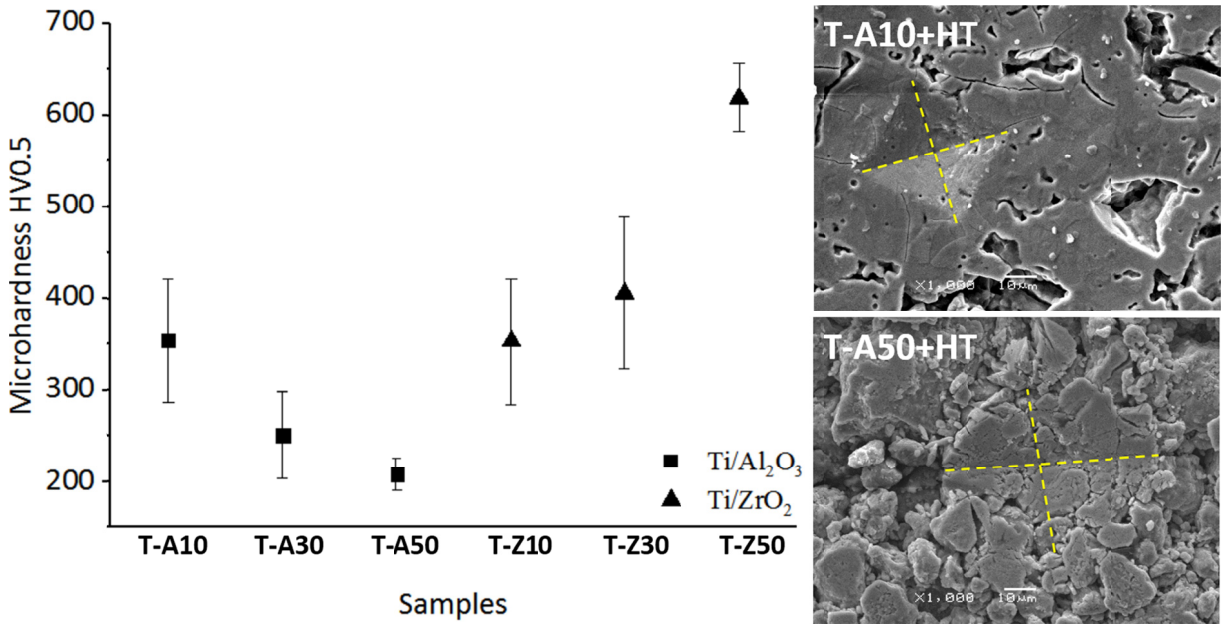

Fig. 6. Microhardness of the T-A10+HT, T-A30+HT, T-A50+HT, T-Z10+HT, T-Z30+HT and T-Z50+HT samples and representative indentations after microhardness measurements for T-A10+HT and T-A50+HT samples

REFERENCES

[1] K. Lee, S.B. Goodman, Current state and future of joint replacements in the hip and knee, Expert Rev. Med. Devices. **5**, 383-393 (2008).

[2] M. Long, H.J. Rack, Titanium alloys in total joint replacement – a materials science perspective, Biomaterials. **19** (18), 1621-1639 (1998).

[3] A.K. Gain, L. Zhang, M.Z. Quadir, Composites matching the properties of human cortical bones: The design of porous titanium-zirconia (Ti-ZrO2) nanocomposites using polymethyl methacrylate powders, Mater. Sci. Eng. A. **662**, 258-267 (2016).

[4] P. Henrique, C. Camargo, K.G. Satyanarayana, F. Wypych, Nanocomposites: Synthesis, Structure, Properties and New Application Opportunities, Mater. Res. **12** (1), 1-39 (2009).

[5] G. Ryan, A. Pandit, D. Apatsidis, Fabrication methods of porous metals for use in orthopaedic applications, Biomaterials. **27** (13), 2651-2670 (2006).

[6] G. He, M. Hagiwara, Bimodal structured Ti-base alloy with large elasticity and low Young's modulus, Mater. Sci. Eng. C. **25** (3), 290-295 (2005).

[7] X. Wang, Y. Chen, L. Xu, S. Xiao, F. Kong, K. Do Woo, Ti-Nb-Sn-hydroxyapatite composites synthesized by mechanical alloying and high frequency induction heated sintering, J. Mech. Behav. Biomed. Mater. **4** (8), 2074-2080 (2011).

[8] L.L. Hench, Bioceramics – from concept to clinic, J. Am. Ceram. Soc. **74** (7), 1487-1510 (1991).

[9] L. Teng, W. Li, F. Wang, Effect of Ti content on the martensitic transformation in zirconia for Ti-ZrO2 composites, J. Alloys Compd. **319** (1-2), 228-232 (2001).

[10] P.F. Manicone, P. Rossi Iommetti, L. Raffaelli, An overview of zirconia ceramics: Basic properties and clinical applications, J. Dent. **35** (11), 819-826 (2007).

[11] M. Inokoshi, F. Zhang, J. De Munck, S. Minakuchi, I. Naert, J. Vleugels, B. Van Meerbeek, K. Vanmeensel, Influence of sintering conditions on low-temperature degradation of dental zirconia, Dent. Mater. **30** (6), 669-678 (2014).

[12] A. Shafiei-Zarghani, S.F. Kashani-Bozorg, A.P. Gerlich, Strengthening analyses and mechanical assessment of Ti/Al_2O_3 nanocomposites produced by friction stir processing, Mater. Sci. Eng. A. **631**, 75-85 (2015).

[13] Z. Yin, C. Huang, B. Zou, H. Liu, H. Zhu, J. Wang, Preparation and characterization of Al2O3/TiC micro-nano-composite ceramic tool materials, Ceram. Int. **39** (4), 4253-4262 (2013).

[14] H.-C. Hsu, S.-C. Wu, S.-K. Hsu, M.-S. Tsai, T.-Y. Chang, W.-F. Ho, Processing and mechanical properties of porous Ti-7.5Mo alloy, Mater. Des. **47**, 21-26 (2013).

[15] C. Caparros, M. Ortiz-Hernandez, M. Molmeneu, M. Punset, J.A. Calero, C. Aparicio, M. Fernandez-Fairen, R. Perez, F.J. Gil, Bioactive macroporous titanium implants highly interconnected, J. Mater. Sci. Mater. Med. **27** (10), 151 (2016).

[16] S. Kujala, J. Ryhänen, A. Danilov, J. Tuukkanen, Effect of porosity on the osteointegration and bone ingrowth of a weight-bearing nickel-titanium bone graft substitute, Biomaterials. **24** (25), 4691-7 (2003).

[17] M. Karolus, J. Panek, Nanostructured Ni-Ti alloys obtained by mechanical synthesis and heat treatment, J. Alloys Compd. **658**, 709-715 (2016).

[18] G. Dercz, I. Matuła, M. Zubko, N. Kuczera, Dispersion and Structure Analysis of Nanocrystalline Ti-m ZrO 2 Composite Powder for Biomedical Applications, J. Nanosci. Nanotechnol. **19** (5), 2799-2806 (2019).

[19] D.B. Wiles, R.A. Young, A new computer program for Rietveld analysis of X-ray powder diffraction patterns, J. Appl. Cryst. **14** (2), 149-151 (1981).

[20] C. Suryanarayana, N. Al-Aqeeli, Mechanically alloyed nanocomposites, Prog. Mater. Sci. **58** (4), 383-502 (2013).

[21] C. Suryanarayana, Mechanical alloying and milling, Prog. Mater. Sci. **46** (1-2), 1-184 (2001).

[22] M.J. Mas-Guindal, E. Benko, M.A. Rodríguez, Nanostructured metastable cermets of Ti-Al_2O_3 through activated SHS reaction, J. Alloys Compd. **454** (1-2), 352-358 (2008).

[23] J. Huaxia, Characterization of the interaction between molten titanium alloy and AI_20_3, J. Mater. Sci. **30**, 5617-5620 (1995).

[24] T.B. Massalski, H. Okamoto, P.R. Subramanian, B. Massalski, L. Thaddeus, Binary Alloy Phase Diagrams, 2nd Ed. ASM International (1990).

[25] H.U.A. Lu, C.L. Bao, D.H. Shen, Y.D. Cui, Z.D. Lin, Study of the Ti / AI_20_3 interface, J. Mater. Sci. **30**, 339-346 (1995).

[26] G. Dercz, I. Matuła, Effect of ball milling on the properties of the porous Ti-26Nb alloy for biomedical applications, Mater. Tehnol. **51** (5), 795-803 (2017).

[27] I.H. Oh, N. Nomura, N. Masahashi, S. Hanada, Mechanical properties of porous titanium compacts prepared by powder sintering, Scr. Mater. **49** (12), 1197-1202 (2003).

[28] V. Karageorgiou, D. Kaplan, Porosity of 3D biomaterial scaffolds and osteogenesis, Biomaterials. **26** (27), 5474-5491 (2005).

[29] L.M.R. Vasconcellos, M. V. Oliveira, M.L.A. Graca, L.G.O. Vasconcellos, C.A.A. Cairo, Y.R. Carvalho, Design of dental implants, influence on the osteogenesis and fixation, J. Mater. Sci. Mater. Med. **19** (8), 2851-2857 (2008).

[30] G. Dercz, I. Matuła, M. Zubko, A. Kazek-Kęsik, J. Maszybrocka, W. Simka, J. Dercz, P. Świec, I. Jendrzejewska, Synthesis of porous Ti-50Ta alloy by powder metallurgy, Mater. Charact. **142**, 124-136 (2018).

[31] A.M. Kliauga, M. Ferrante, Interface compounds formed during the diffusion bonding of Al2O3 to Ti, J. Mater. Sci. **35**(17), 4243-4249 (2000).

[32] J.S. Moya, S. Lopez-Esteban, C. Pecharromán, The challenge of ceramic/metal microcomposites and nanocomposites, Prog. Mater. Sci. **52** (7), 1017-1090 (2007).

[33] J.S. Moya, S. López-Esteban, C. Pecharromán, J.F. Bartolomé, R. Torrecillas, Mechanically stable monoclinic zirconia-nickel composite, J. Am. Ceram. Soc. **85** (8), 2119-2121 (2002).

[34] M.U. Jurczyk, K. Jurczyk, K. Niespodziana, A. Miklaszewski, M. Jurczyk, Titanium-SiO_2 nanocomposites and their scaffolds for dental applications, Mater. Charact. **77**, 99-108 (2013).